Nuclear Instruments and Methods in Physics Research B 308 (2013) 80–87

Contents lists available at SciVerse ScienceDirect

Nuclear Instruments and Methods in Physics Research B

journal homepage: www.elsevier.com/locate/nimb

Molecular dynamics simulation of erosion and surface evolution of tungsten due to bombardment with deuterium and carbon in Tokamak fusion environments

Xue Yang *, Ahmed Hassanein

Center for Material under Extreme Environment, School of Nuclear Engineering, Purdue University, West Lafayette, IN 47907, USA

ARTICLE INFO

Article history:
Received 8 March 2013
Received in revised form 13 May 2013
Available online 24 May 2013

Keywords:
Molecular dynamic simulation
Carbon irradiation on tungsten
Simultaneous carbon and deuterium bombardment
Hydrogen bubble formation
Tungsten sputtering yield

ABSTRACT

The behavior of tungsten as plasma facing material in fusion environment is investigated using molecular dynamics simulation. Tungsten erosion and surface evolution is simulated during irradiation by carbon and deuterium ions. Non-cumulative pure carbon bombardment on crystal tungsten shows that substrate temperature does not affect carbon trapping rate, implantation depth, and tungsten sputtering yield. Carbon induced tungsten physical sputtering yield threshold is predicted to be around ~25 eV. Cumulative carbon irradiation on crystal tungsten reveals that tungsten erosion is enhanced at high substrate temperatures. Cumulative carbon induced tungsten sputtering yield matches experimental data as well as Monte Carlo results. Carbon pre-irradiated tungsten tends to trap more hydrogen and facilitates gas bubble formation. Simultaneous deuterium and carbon bombardment on crystal tungsten indicates that carbon induced tungsten sputtering yield exhibits a maximum value when carbon ratio is around 20%. Higher carbon ratio reduces both the carbon and deuterium trapping rates.

Published by Elsevier B.V.

1. Introduction

Tungsten and carbon fiber composites (CFCs) are plasma-facing components (PFCs) candidates in ITER where they are subjected to high hydrogen plasma fluxes. For carbon-based materials (CBM), chemical interactions with hydrogen isotopes lead to enhanced erosion yield [1], especially at elevated surface temperature (~0.1 at 600–800 K) [2]. Erosion rate of CBM during normal fusion reactor operation is several meters per year [1]. The eroded carbon atoms can migrate to other places and re-deposit on tungsten surface to form thin carbon film and remove tungsten atoms from the surface. The deposited carbon on tungsten surface increases hydrogen retention, which was mainly confined to the carbon-modified layer [3,4], and hydrogen concentration in the carbon deposited layer depends on the incident hydrogen energy: energetic ions lead to hard films with lower hydrogen concentration, while low energy hydrogen leads to soft films with higher hydrogen concentration [5,6]. Computer simulations reveal that hydrogen isotopes bubble could be formed in tungsten carbide, if sufficient high amount of D_2 accumulates in the substrate [7]. The consequences of these complicated processes will result in tungsten dust in the plasma [8]. The dust is formed either directly from erosion process causing ejection of particulates, or by delamination of re-deposited layers. Because tungsten impurities in fusion plasma need to be significantly minimized due to plasma power loss by line radiation from charge states [8], understanding detailed tungsten surface evolution during deuterium bombardment with carbon impurity is crucial for the usage of tungsten and CFCs in fusion reactors.

One of the principal tools in theoretical study of molecular/atomic systems is the method of molecular dynamics (MD) simulations. The trajectories of physical movements of atoms and molecules are determined by Newton's equation of motion in the classical MD simulation. MD simulations have been used for investigating various fields of plasma material interaction. Hydrogen or helium implantation on tungsten or other fusion relevant materials has been studied using MD simulations [9–21]. For MD simulations involving hydrogen, carbon, and tungsten, most of the simulations model the hydrogen bombardment on crystalline tungsten carbide [22–26]. Depth profiles, snapshot of damage, carbon and tungsten sputtering yield, surface atomic concentration, blister formation, H trapping and reemission rate, can be acquired using MD simulations. Little effort is devoted to MD simulation of deuterium bombardment on amorphous WC with relatively limited results and analysis [14,22,27]. This work mainly focus on carbon bombardment, simultaneous deuterium and carbon implantation on crystalline tungsten and deuterium bombardment on tungsten pre-irradiated by carbon to study the effect of carbon impurity in fusion plasma on tungsten surface.

* Corresponding author. Tel.: +1 765 404 9997.
E-mail address: yang99@purdue.edu (X. Yang).

0168-583X/$ - see front matter Published by Elsevier B.V.
http://dx.doi.org/10.1016/j.nimb.2013.05.012

2. Simulation method

The following simulations were performed using the classical LAMMPS computer code [28]. The W–C–H analytic bond-order potential [29] was converted to LAMMPS Tersoff type interatomic potential to describe the ternary W–C–H system of bulk, surface, and projectiles [19]. The cohesive energy and lattice parameter of tungsten bulk, the cohesive energy and bond length/angle of WH_x and WC molecules, cohesive energy, lattice parameter, axial ratio and unit cell volume of tungsten carbide are computed by LAMMPS. LAMMPS results match PARCAS results [29] well indicating correct conversion.

The initial substrate is crystalline body centered cubic (bcc) tungsten with a size of 8 by 8 by 55 lattices along *x*, *y*, and *z* direction. The origin is placed at one corner of the top surface. A lattice parameter of 3.165 Å was used to construct the tungsten sample, because it yields minimum potential energy [19]. The side boundary conditions are set to periodic, while the top and bottom boundary conditions are set to non-periodic and fixed (if an atom moves outside the boundary, it will be removed from the system). The bottom three layers of atoms are fixed in the space to withstand the momentum of energetic ions. Prior to the bombardment, the mobile tungsten atoms are assigned an initial velocity with a Gaussian distribution according to the desired sample temperature. Then, the temperature rescaling is performed for 1000 steps using 0.01 ps as step size to reach the temperature equilibrium.

During the bombardment, two layers of the tungsten atoms above the fixed atoms and one layer surrounding the side of the tungsten bulk were maintained at the desired temperature using Berendsen thermostat. The temperature is set to relax in a time span of 0.01 ps. The projectile is randomly placed 10 lattice parameters (31.65 Å) above the sample initial top surface with specific energy (velocity), so that after all bombardment, the projectile initial position will still be above the deposited layer. The polar angle of ion initial travelling direction is randomly selected between 0° and 20° off normal downward, while the azimuthal angle is uniformly distributed on *X*–*Y* plane. For cumulative bombardment, system will generate a new ion every 2.5 ps (5000 time steps), resulting in a flux of 6.2×10^{28} m^{-2} s^{-1}, which is used for all cumulative bombardments.

3. Results and discussion

3.1. Non-cumulative carbon implantation on tungsten

To investigate the initial damage to tungsten by carbon impinging, non-cumulative carbon bombardment on tungsten is simulated. These series of simulations direct 50, 100, 150, 200 or 250 eV carbon atoms to 300, 600, 1000 or 1500 K tungsten samples. Each run impinges 5000 carbon ions into the substrate. If the carbon atom is trapped in the substrate, this event is recorded. If the carbon escapes from the upper simulation boundary, the simulation is restarted with a new incoming carbon atom.

The carbon-trapping rate is defined as the total number of carbon atoms trapped in tungsten sample divided by the total number of incident carbon ions (5000). Carbon-trapping rate of non-cumulative bombardment is shown in Fig. 1. The increasing trend exhibits a logarithm type. Energetic incoming ions have larger penetration depth, and are more likely to be trapped in the substrate. The tungsten temperature barely affects the trapping rate. This phenomenon is different from the deuterium retention rate predicted by MD simulation, which reveals that higher tungsten temperature increases the deuterium retention rates [19,26], due to lattice recrystallization process [26]. Because carbon forms strong bond with tungsten, but hydrogen is highly mobile in tungsten, this process barely affects carbon trapping.

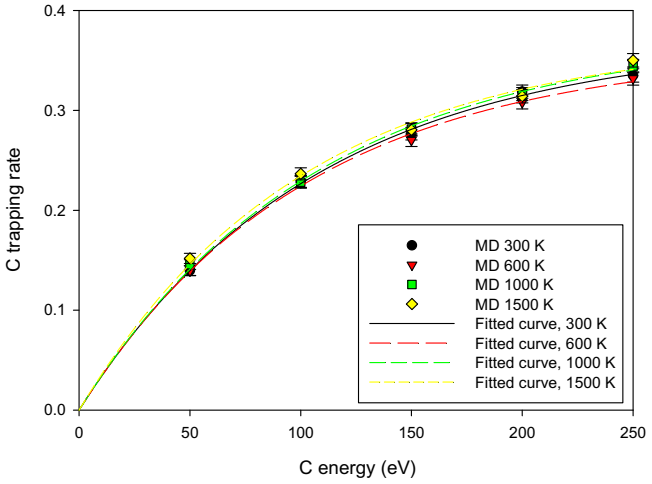

Fig. 1. Carbon trapping rates of non-cumulative pure carbon bombardment on crystalline tungsten; carbon energy: 50, 100, 150, 200 and 250 eV; tungsten temperature: 300, 600, 1000 and 1500 K; number of projectiles: 5000 per run.

If a carbon atom is trapped in the substrate to become an interstitial atom, the depth of such atom is recorded. Fig. 2 depicts the depth profiles of non-cumulative bombardment. The counts are collected into multiple bins with a width of 3 Å. Energetic projectiles clearly reach higher depth. The substrate temperature barely affects the depth distribution. Compared to the 300 K results, the depth peaks of 1500 K move towards *Z* positive direction for 3 Å, but it is insignificant to conclude any temperature effect. The negative depth in Fig. 2 means the incoming carbon ions land on the tungsten surface.

If any tungsten atom is no longer bonded to substrate and travels across the upper boundary of the simulation box, such atom is considered sputtered. The tungsten sputtering yield is defined as the total number of sputtered tungsten atoms divided by the total number of incident carbon atoms (5000). Fig. 3 shows tungsten sputtering yield as a function of the incident carbon energy. The trends are relatively linear with the incident energy for this energy range. From the extrapolation, the sputtering threshold energy is around 25 eV.

3.2. Cumulative carbon implantation on tungsten

To further investigate tungsten erosion by carbon, the simulations of cumulative carbon implantation on tungsten are carried out using MD simulation. In these simulations, the tungsten samples with temperature of 300, 600, 1000 and 1500 K are repeatedly bombarded by 3000 carbon ions with energies of 100 or 200 eV. The equivalent fluence is about 5.0×10^{20} m^{-2}.

Fig. 4 illustrates the tungsten erosion by cumulative carbon bombardment. The surface layer is damaged by the incoming carbon and become amorphous tungsten carbide. The carbon ratio in the surface layer increases with fluence. At the end of the bombardment, the carbon atom ratio in the surface amorphous layer is about 0.25–0.35. The surface amorphous layer density decreases with fluence. At the end of the bombardment, the surface amorphous layer density reaches 10–14 g cm^{-3} (tungsten density: 19.3 g cm^{-3}; amorphous carbon density: 1.8–2.1 g cm^{-3}). The erosion of 200 eV carbon is about 5 Å higher than the one of 100 eV carbon, while the carbon deposited layer of the 100 eV bombardment swells toward the *z* positive direction.

The curves in Fig. 5 represent the number of remaining tungsten atoms in the substrate. The upper four curves are the results of 100 eV carbon bombardment, while the lower four curves are the

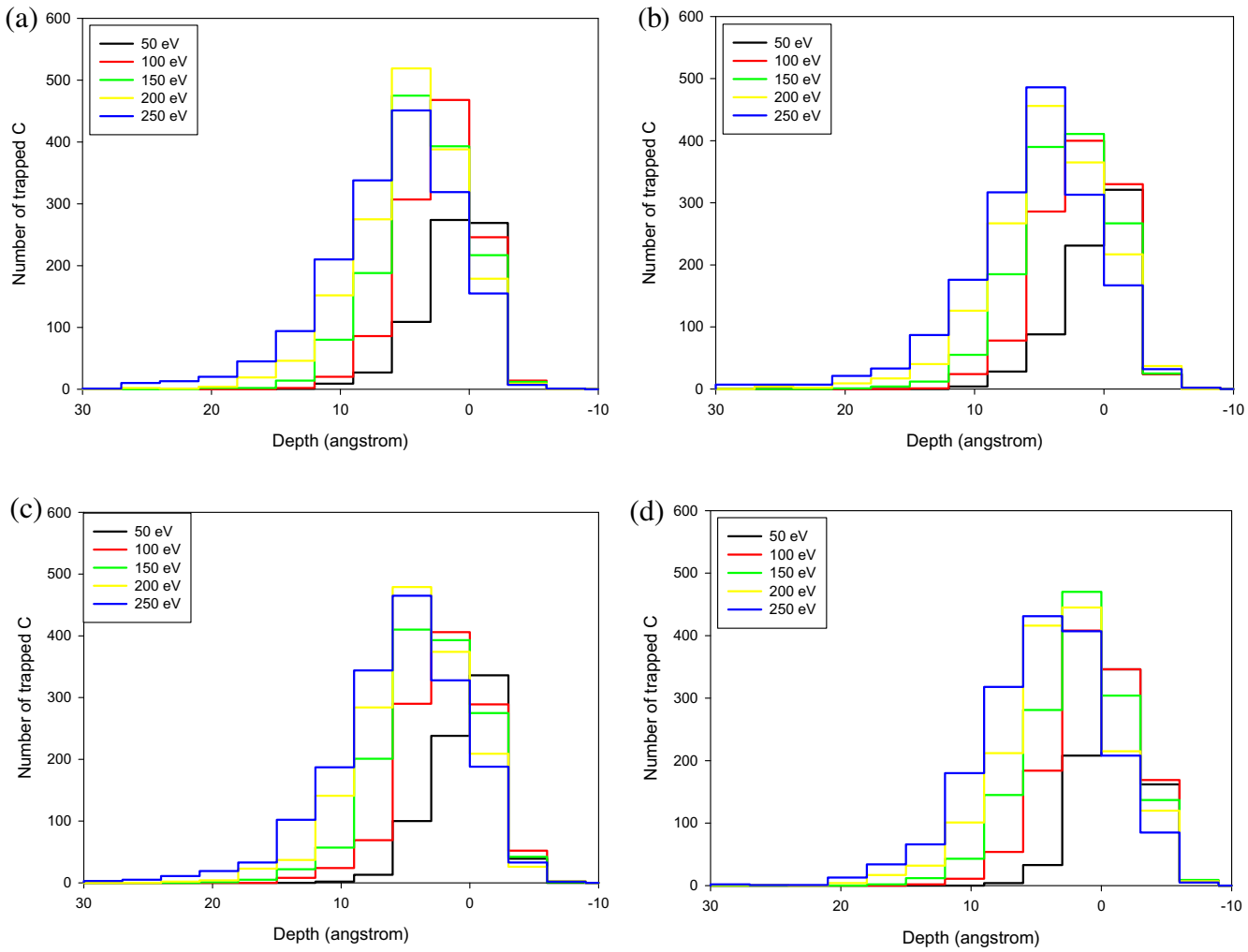

Fig. 2. Carbon depth profiles of non-cumulative carbon bombardment on tungsten. (a): 300 K; (b): 600 K; (c): 1000 K; (d): 1500 K. Bin size: 3 Å.

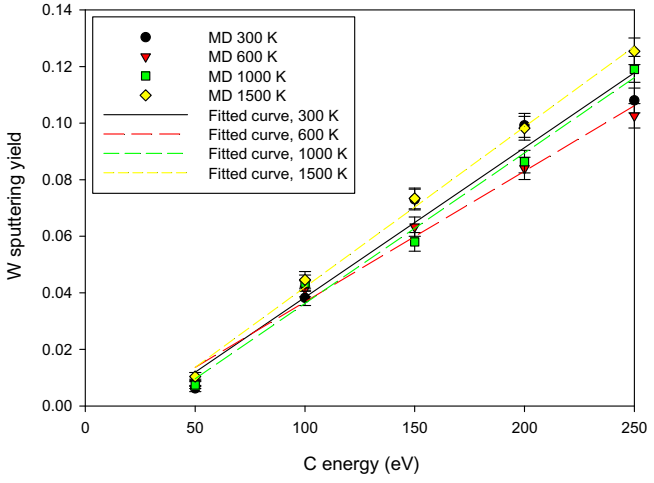

Fig. 3. Non-cumulative carbon bombardment induced tungsten sputtering yield.

results of 200 eV carbon bombardment case. Fig. 5 shows that tungsten keeps losing its weight till the end of simulations. Both theoretical erosion formula and experiments suggest when tungsten is bombarded by carbon ions, the sample will first lose its weight because the tungsten is sputtered by the incoming carbon ions. Then, the sample weight will keep increasing after the pure surface carbon film is formed and carbon deposition prevails [32]. Due to the limitation of MD simulation, the simulated fluence is several magnitudes lower than that of the performed experiments. Therefore, our MD simulation only demonstrates the initial tungsten weight loss phase.

As also shown in Fig. 5, the erosion rates of the 200 eV carbon bombardments are about 3–5 times larger than the ones of the 100 eV bombardments. Higher substrate temperature clearly enhances the erosion. Due to reduced surface binding energy [35,42], high substrate temperature increases C self-sputtering, which is responsible for the enhanced W erosion, because the tungsten surface is less shielded by the C layer [35]. Experiments [34] and Monte Carlo simulations (TRIDYN) [35] of 6 keV carbon ion implantation on tungsten present similar phenomena, i.e., the tungsten sputtering yield at 870 K is about twice times higher than that of room temperature.

After bombardment of 3000 carbon ions, tungsten sputtering yield is calculated and plotted as shown in Fig. 6. Compared to the non-cumulative bombardment results, the sputtering yield of cumulative bombardment is lower. Because a carbon layer is formed at the tungsten surface, and the tungsten atom ratio in the surface layer keeps decreasing, the incoming carbon ions have less chance to interact with tungsten atom, and the beneath tungsten bulk is protected by the enriched surface carbon layer. Therefore, tungsten sputtering yield by the cumulative carbon

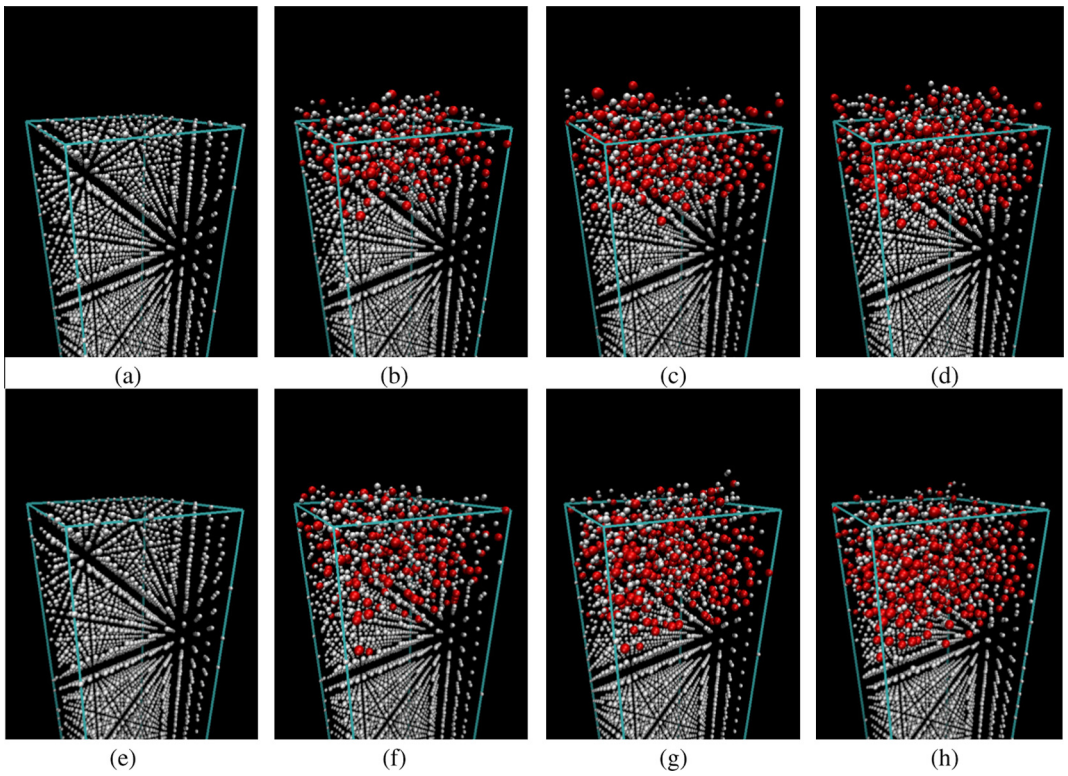

Fig. 4. Snapshots of the 300 K tungsten erosion during cumulative carbon bombardment process. (a)–(d): incident carbon energy: 100 eV, snapshots of substrate after 0, 1000, 2000, and 3000 impacts; (e)–(h): incident carbon energy: 200 eV, snapshots of substrate after 0, 1000, 2000, and 3000 impacts. White: tungsten atoms; red: carbon atoms. (For interpretation of the references to colour in this figure legend, the reader is referred to the web version of this article.).

bombardment is lower than that by the non-cumulative bombardment. In addition, we compared the 100 eV carbon induced tungsten sputtering at 300 K with other's MD result based on the same potential and EDDY Monte Carlo solution [25]. Their MD and EDDY solutions both give a tungsten sputtering yield of ~0.02 at fluence of 5×10^{20} m^{-2}, which is in good agreement with our results.

The trapped carbon depth profiles of 300 K case after 1000, 2000, and 3000 impacts are presented in Fig. 7. Both 100 and 200 eV results show that the carbon deposition grows towards the Z negative direction, indicating some trapped carbons are pushed deeper by the subsequent bombardment, and the tungsten sample is not affected by the cumulative carbon implantation beyond certain depth.

3.3. Deuterium bombardment on tungsten pre-irradiated by carbon

Before deuterium bombardment, the tungsten sample is pre-irradiated by 3000 carbon ions with energy of 100 eV. At the end of the carbon pre-irradiation, there are about 300 carbon atoms (atomic ratio: 41%) in the surface amorphous layer ranging roughly from $z = -13$–5 Å. The estimated surface layer density is 13.2 g cm^{-3}. Then, it is subjected to 10 or 100 eV deuterium bombardment. The simulation is terminated upon 5000 deuterium

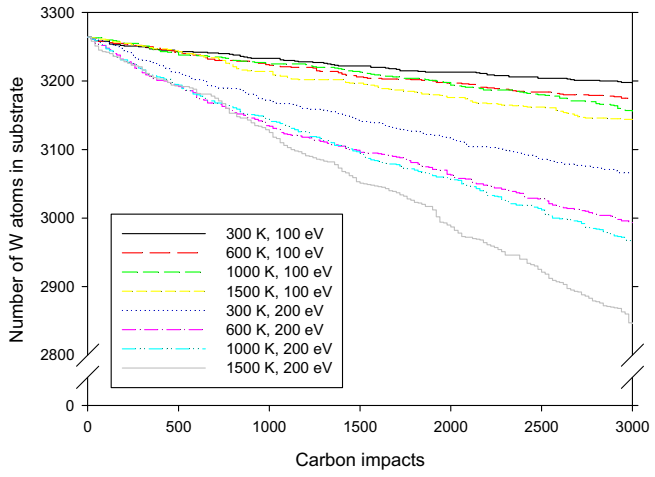

Fig. 5. Number of remaining W in the substrate during cumulative carbon bombardments.

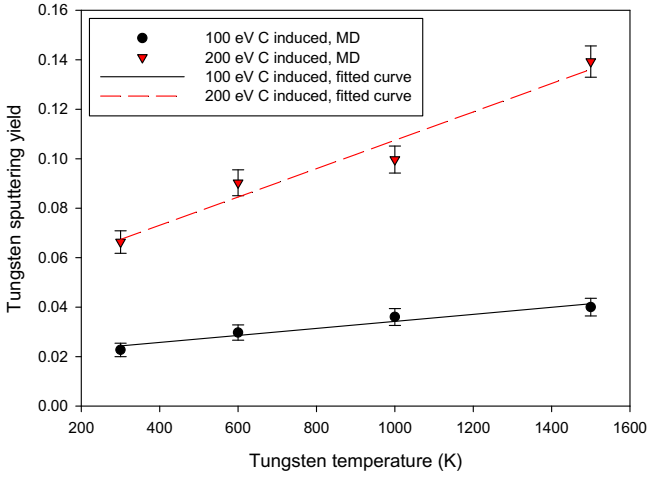

Fig. 6. Cumulative carbon bombardment induced tungsten sputtering yield. Incoming carbon energies: 100 and 200 eV.

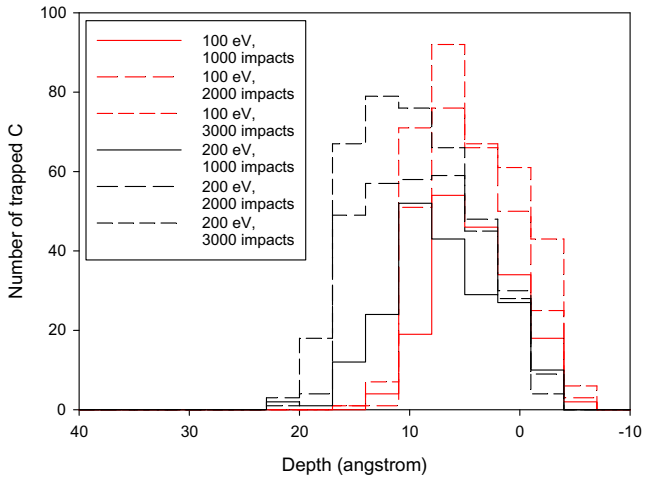

Fig. 7. Depth profiles of cumulative carbon bombardments on 300 K tungsten after 1000, 2000 and 3000 impacts. Carbon energies: 100 eV (red lines) and 200 eV (black lines). Bin size: 3 Å. (For interpretation of the references to colour in this figure legend, the reader is referred to the web version of this article.).

implantation or the formation of a gas bubble; whichever comes first. The tungsten sample is maintained at 300 K at all time.

The10 eV deuterium case barely modifies the substrate surface. No tungsten atom is removed, and only 2 carbon atoms are sputtered. There are only 72 deuterium atoms trapped in the substrate (trapping rate: 0.0144). For the 100 eV deuterium bombardments, no tungsten atom is removed either, because the incoming deuterium energy is well below the tungsten displacement threshold (940 eV for deuterium [30]). Fig. 8 presents the number of remaining carbon and the number of trapped deuterium in the substrate. After around 2050 deuterium impacts, both carbon and deuterium inventories in the sample have a sudden drop, because a gas bubble is formed and the bubble cap is separated from the sample and flew away, causing sudden loss of a large amount of atoms. The deuterium induced carbon sputtering yield right after 2000 impacts is 0.117, and about one third of the incoming deuterium atoms are trapped in the sample. Experiments of deuterium implantation into tungsten carbide also indicate that the C atoms in WC were selectively sputtered by D_2 + implantation [33].

Fig. 9 illustrates the gas bubble formation process. Analysis of snapshots reveals that more than one half of the trapped deuterium stays in the surface amorphous WC layer. After 2000 impacts,

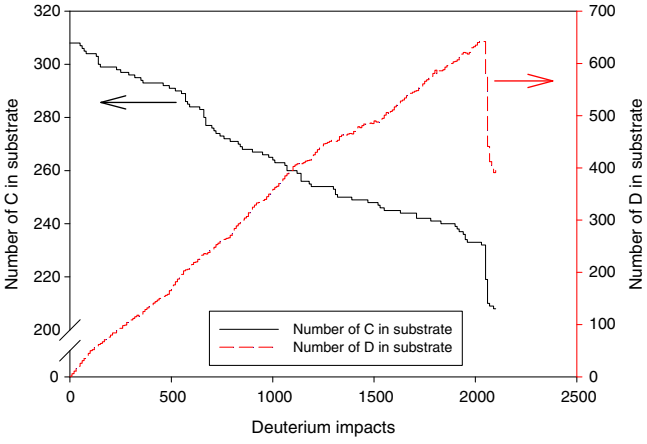

Fig. 8. Number of carbon and deuterium atoms in the substrate for simulation of 100 eV deuterium implantation on tungsten pre-irradiated by 100 eV carbon ions.

57% of the trapped deuterium atoms are within the surface amorphous layer ($z > -13$ Å). This phenomenon also matches previous findings from experiments: large amount of hydrogen is confined within the surface WC layer [3,4]. Large amount of D_2 molecules also formed within the amorphous layer. Assuming the D–D bond length is about 0.74 Å, the number of D_2 molecules can be calculated. After 1000 and 1500 impacts, in the surface amorphous layer, about 35% deuterium atoms are in D_2 molecule form, while the D_2 ratio slightly drops to 29%, after 2000 impacts. MD simulation shows deuterium usually appears in atomic form in crystalline tungsten, while large amount of D_2 can be formed when crystalline WC is bombarded by deuterium [26]. Our MD results also confirm that: when pure crystalline tungsten is bombarded by deuterium, only about 2% trapped deuterium is in D_2 form [19]. Experiments show that the surface carbon film will increase the deuterium trapping rate and the deuterium is mainly trapped within the surface carbon film [3], facilitating bubble formation, because D is preferentially trapped by C, vacancies and interstitial sites in amorphous layer [33], preventing it from migrating to deeper bulk regions. Our ITMC-DYN Monte Carlo results also shows that increasing carbon concentration in the surface layer can significantly decreases the diffusion coefficient of hydrogen isotopes to increase hydrogen retention within the surface layer [36]. The sample evolution in our MD simulations shows similar trends: no bubble was found when crystalline tungsten was bombarded by 5000 deuterium ions [19], while gas bubble formed as early as 2000 deuterium bombardment in amorphous WC layer.

Hydrogen implantation induced bubbles are found on the surfaces of many types of metals and alloys [37], and recent experiments are focusing on tungsten surface blistering effect [3,38–41]. However, it should be noted that the deuterium bubble formation based on cumulative bombardment could not be directly compared with the experiment, because of the high deuterium flux used in the simulation, which is several magnitudes higher than the actual condition. The hydrogen blister found on tungsten surface in the experiment involves the diffusion effect, which does not play an important role in these MD simulations, due to the very short of simulated timescale [7]. However, the bubble formation mechanism is similar in both MD simulations and experiment: the high gas pressure caused by near surface hydrogen supersaturation results in tungsten plastic deformation [37].

3.4. Simultaneous deuterium and carbon bombardment on tungsten

To study the effect of mixed materials and impurity bombardment for more realistic fusion reactor environment, we simulated the simultaneous bombardment of deuterium and carbon mixture on crystalline tungsten. Each simulation directs 5000 ions of 10 eV deuterium or 100 eV carbon into 300 K tungsten sample. The carbon ratios used in the ion mixture are 1%, 10%, 20%, 50%, 80%, 90% and 99%. All other configurations are identical to the simulations described in previous sections. Fig. 10 shows the number of tungsten atoms remaining in the substrate for different carbon concentration. The tungsten erosion rate is enhanced by higher carbon concentration.

Because only carbon could remove tungsten atom, and 10 eV deuterium could not displace tungsten atom, the tungsten-sputtering yield is defined as the number of lost tungsten atoms divided by the number of incoming carbon. The results are plotted in Fig. 11. The sputtering yield exhibits a maximum value when the carbon ratio reaches about 20%. This phenomenon can be explained as follows: if the carbon ratio is high and approaches 100%, the tungsten sputtering yield will be close to that of pure carbon cumulative bombardment discussed in the previous section, and the sputtering will be suppressed by the surface deposited carbon layer, which is also seen in recent experiments using

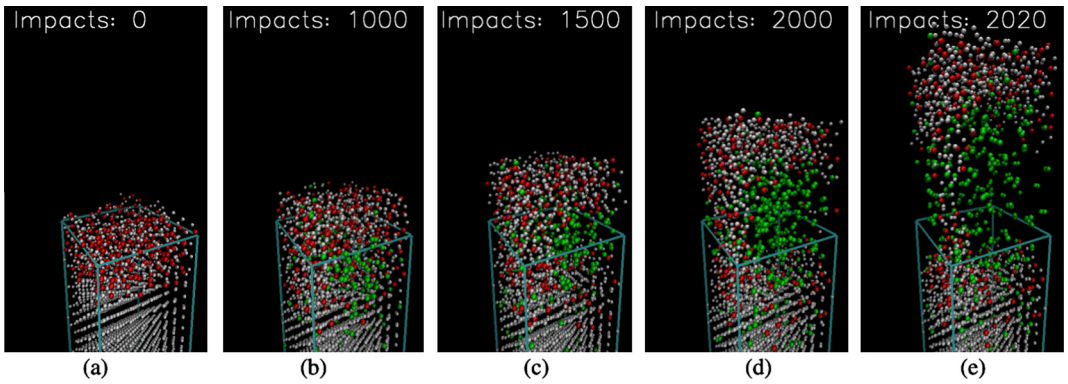

Fig. 9. Snapshots of the 100 eV deuterium bombardments on tungsten pre-irradiated by 100 eV carbon. (a–e): snapshots after 0, 1000, 1500, 2000, and 2020 deuterium impacts. White: tungsten; red: carbon; green: deuterium.

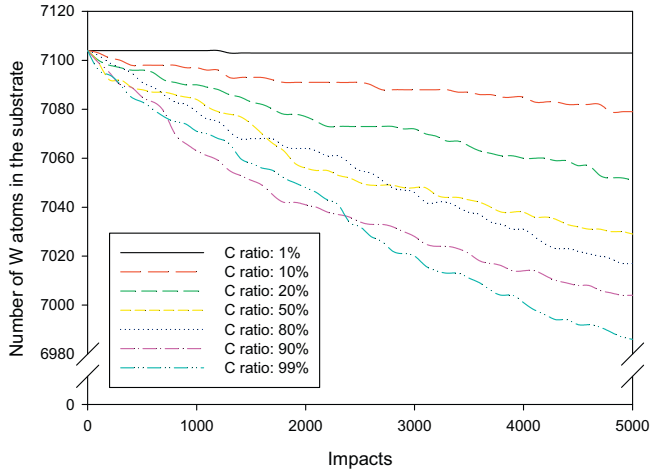

Fig. 10. Number of tungsten atoms in 300 K tungsten substrate for various carbon ratios in the mixture of deuterium and carbon ions.

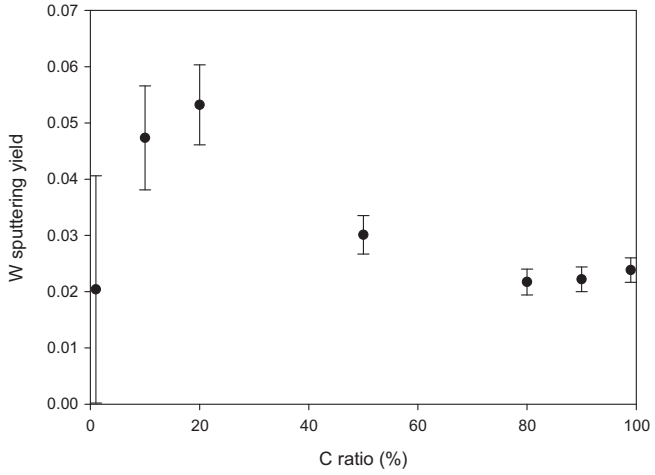

Fig. 11. Carbon induced tungsten sputtering yield for simultaneous 10 eV deuterium and 100 eV carbon bombardment on 300 K tungsten. (Number of sputtered tungsten divided by number of incident carbon).

simultaneous impact of carbon and hydrogen ions (CH_3^+) causing carbon film build up on tungsten surface at room temperature [31]. However, if the carbon ratio is very low, the projected carbon may interact with the trapped deuterium to lose its kinetic energy, because the deuterium content in the substrate is relatively high.

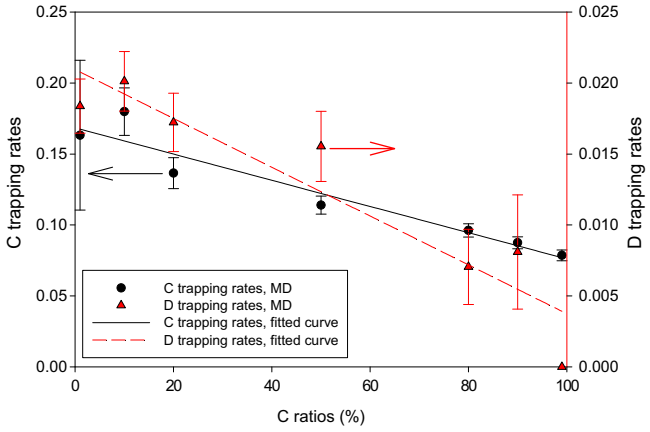

Fig. 12. Carbon and deuterium trapping rates of simultaneous 10 eV deuterium and 100 eV carbon bombardment on 300 K tungsten.

Therefore, the tungsten sputtering caused by low carbon concentration bombardment is lower than the results of the non-cumulative carbon bombardment, due to the presence of the deuterium in the substrate.

At the end of each simulation, the carbon and deuterium trapping rates is calculated and plotted in Fig. 12. The trend shows that carbon and deuterium trapping rates are low when carbon ratio is high. As mentioned in previous sections, the carbon trapping rate of non-cumulative bombardment is higher than that of the cumulative bombardment. Therefore, the carbon trapping rate of the low carbon ratio is higher, because the surface carbon film is not well formed, and carbon self-sputtering is not significant. More deuterium atoms could migrate to the bulk region, because there are not many vacancies at the surface caused by amorphization. Therefore, both C and D trapping rates are higher. If C ratio is high, the deposited carbon tends to be removed by C self-sputtering process. Therefore, carbon trapping rate for the high carbon ratio is relatively lower. For higher carbon ratios, the deuterium ions have higher chance to interact with deposited carbon and form hydrocarbon and leave the tungsten sample, leading to relatively low deuterium trapping rate.

4. Conclusion

The effect of hydrogen isotope and impurity bombardment of tungsten as plasma facing material in more realistic fusion environment is studied. A series of MD simulation based on a Tersoff type interatomic potential is performed to investigate the tungsten

erosion process during both carbon and deuterium bombardment. Non-cumulative 50–250 eV carbon bombardment on 300–1500 K tungsten was first simulated. Substrate temperature has no effect on carbon trapping rate, depth profiles, and tungsten sputtering yield. The threshold of carbon induced tungsten sputtering predicted by MD is ~25 eV. Tungsten erosion process is then studied by cumulative carbon implantation on tungsten. Tungsten samples of 300–1500 K are repeatedly bombarded by 100 or 200 eV carbon ions. Tungsten erosion rate is enhanced by the substrate temperature, because higher temperature increases C self-sputtering and tungsten surface is not well protected by the C deposited layer. This phenomenon also matches previous findings from both experiments and Monte Carlo simulations, showing that tungsten sputtering at 870 K is about two times higher than that at room temperature. There is also good agreement of the tungsten sputtering yield between our MD simulation and other MD and Monte Carlo results at fluence of 5×10^{20} m^{-2}.

Deuterium bombardment on carbon pre-irradiated tungsten was also modeled using MD simulations. Deuterium ions of 10 eV implantation barely change the substrate surface, while deuterium of 100 eV implantation forms a gas bubble within the surface amorphous WC layer. The deuterium retention rate is increased by the surface amorphous WC layer, because hydrogen is preferentially trapped by C, vacancies, and interstitial sites in amorphous layer. The bubble formation is facilitated by the WC layer. As a comparison, our previous MD simulation shows that no bubble is formed in 300 K crystal tungsten after 5000 deuterium ion implantation. More than one half of the trapped deuterium is confined in the WC layer, matching the recent experimental findings. About 30% of trapped deuterium atoms are in the form of D_2, while the D_2 rate is only ~2% in the MD modeling of deuterium bombardment on crystalline tungsten. To simulate the effect of mixed materials and impurities in more realistic fusion environment, we modeled the simultaneous carbon and deuterium impinging on crystalline tungsten with various ion mixture ratios. Carbon induced tungsten sputtering yield exhibits a maximum value, when carbon ratio is 20%. Higher carbon ratio leads to surface carbon film, protecting the tungsten sample beneath. While for lower carbon ratio, the incoming carbon may interact with the large amount of trapped hydrogen instead of tungsten. In addition, higher carbon ratio results in lower carbon and deuterium retention rates, because WC surface layer may be formed when carbon ratio is high. The abundant carbon at the surface may be removed by C self-sputtering, and the incoming deuterium may combine with the deposited carbon to form hydrocarbon and leave the surface. Therefore, both carbon and deuterium trapping rates are reduced in the high carbon ratio scenario. It should be noted that the results from cumulative bombardment MD simulation cannot be directly compared with experiment data, because of the high flux used in these simulations, which is several orders higher than the real condition. Due to the very short period of simulated time, the diffusion process was not taken into account. Therefore, these results present only qualitative analysis and, at this time, could only be compared to other MD and MC work as described in the manuscript.

Acknowledgements

This work is partially supported by the US Department of Energy, Office of Fusion Energy Sciences.

References

[1] J. Roth, J. Bohdansky, W. Poschenrieder, M.K. Sinha, Physical and chemical sputtering of graphite and sic by hydrogen and helium in the energy range of 600 to 7500 eV, J. Nucl. Mater. 63 (1976) 222–229.
[2] J. Roth, E. Tsitrone, A. Loarte, Th. Loarer, G. Counsell, R. Neu, V. Philipps, S. Brezinsek, M. Lehnen, P. Coad, Ch. Grisolia, K. Schmid, K. Krieger, A. Kallenbach, B. Lipschultz, R. Doerner, R. Causey, V. Alimov, W. Shu, O. Ogorodnikova, A. Kirschner, G. Federici, A. Kukushkin, EFDA PWI task force, ITER PWI team, fusion for energy, ITPA SOL/DIV, recent analysis of key plasma wall interactions issues for ITER, J. Nucl. Mater. 390–391 (2009) 1.
[3] V.Kh. Alimov, J. Roth, R.A. Causey, D.A. Komarov, Ch. Linsmeier, A. Wiltner, F. Kost, S. Lindig, Deuterium retention in tungsten exposed to low-energy, high-flux clean and carbon-seeded deuterium plasmas, J. Nucl. Mater. 375 (2008) 192–201.
[4] V. Kh Alimov, K. Ertl, J. Roth, K. Schmid, Retention of ion-implanted deuterium in tungsten pre-irradiated with carbon ions, J. Nucl. Mater. 282 (2000) 125–130.
[5] T. Schwarz-Selinger, A. von Keudell, W. Jacob, Plasma chemical vapor deposition of hydrocarbon films: the influence of hydrocarbon source gas on the film properties, J. Appl. Phys. 86 (1999) 3988.
[6] W. Jacob, Surface reactions during growth and erosion of hydrocarbon films, Thin Solid Films 326 (1998) 1.
[7] Katharina Vörtler, Kai Nordlund, Molecular dynamics simulations of deuterium trapping and re-emission in tungsten carbide, J. Phys. Chem. C 114 (2010) 5382–5390.
[8] R.E. Nygren, R. Raffray, D. Whyte, M.A. Urickson, M. Baldwin, L.L. Snead, Making tungsten work – ICFRM-14 session T26 paper 501, J. Nucl. Mater. 417 (2011) 451.
[9] K.O.E. Henriksson, K. Nordlund, J. Keinonen, Molecular dynamics simulation of helium cluster formation in tungsten, Nucl. Instrum. Meth. B 244 (2006) 377.
[10] K.O.E. Henriksson, K. Nordlund, J. Keinonen, D. Sundholm, M. Patzschke, Simulations of the initial stages of blistering in helium implanted tungsten, Phys. Scr. T108 (2004) 95–98.
[11] Z. Insepov, A. Hassanein, Molecular dynamics simulation of Li surface erosion and bubble formation, J. Nucl. Mater. 337–339 (2005) 912–916.
[12] Kaoru Ohya, Naohide Mohara, Kensuke Inai, Atsushi Ito, Hiroaki Nakamura, Yoshio Ueda, Tetsuo Tanabe, Molecular dynamics study of plasma surface interactions for mixed materials, J. Plasma Fusion Res. SERIES (2010) 497.
[13] Z. Yang, Q. Xu, R. Hong, Q. Li, G. Luo, Molecular dynamics simulation of low-energy atomic hydrogen on tungsten surface, Fusion Eng. Des. 85 (2010) 1517–1520.
[14] K. Ohya, N. Mohara, K. Inai, A. Ito, H. Nakamura, A. Kirschner, D. Borodin, Molecular dynamics and dynamic Monte Carlo studies of mixed materials and their impact on plasma wall interactions, Fusion Eng. Des. 85 (2010) 1167–1172.
[15] O.H.Y.A. Kaoru, I.N.A.I. Kensuke, K.I.K.U.H.A.R.A. Yasuyuki, N.A.K.A.N.O. Tomohide, K.A.W.A.T.A. Jun, K.A.W.A.Z.O.M.E. Hayato, U.E.D.A. Yoshio, T.A.N.A.B.E. Tetsuo, Transport of heavy hydrocarbon and its redeposition on plasma facing walls, J. Plasma Fusion Res. SERIES 8 (2009) 419–424.
[16] Xiao-Chun Li, F. Gao, Guang-Hong Lu, Molecular dynamics simulation of interaction of H with vacancy in W, Nucl. Instrum. Methods 267 (2009) 3197–3199.
[17] K.O.E. Henriksson, K. Nordlund, A. Krasheninnikov, J. Keinonen, The depths of hydrogen and helium bubbles in tungsten: a comparison, Fusion Sci. Technol. 50 (2006) 43–57.
[18] K.O.E. Henriksson, K. Vörtler, S. Dreißigacker, K. Nordlund, J. Keinonen, Sticking of atomic hydrogen on the tungsten (001) surface, Surf. Sci. 600 (2006) 3167–3174.
[19] X. Yang, A. Hassanein, Molecular dynamics simulation of deuterium trapping and bubble formation in tungsten, J. Nucl. Mater. 434 (2012) 1–6.
[20] E. Salonen, K. Nordlund, J. Keinonen, C.H. Wu, Molecular dynamics studies of the sputtering of divertor materials, J. Nucl. Mater. 313–316 (2003) 404–407.
[21] I.S. Landman, H. Wuerz, Molecular dynamics simulations of the effect of deuterium on tungsten erosion by oxygen, J. Nucl. Mater. 313–316 (2003) 77–81.
[22] P. Träskelin, N. Juslin, P. Erhart, K. Nordlund, Molecular dynamics simulations of hydrogen bombardment of tungsten carbide surfaces, Phys. Rev. B 75 (2007) 174113.
[23] K. Vörtler, C. Björkas, K. Nordlund, The effect of plasma impurities on the sputtering of tungsten carbide, J. Phys. Condens. Matter 23 (2011) 085002.
[24] P. Träskelin, C. Björkas, N. Juslin, K. Vörtler, K. Nordlund, Radiation damage in WC studied with MD simulations, Nucl. Instrum. Meth. B 257 (2007) 614–617.
[25] K. Inai, Y. Kikuhara, Kaoru Ohya, Comparison of carbon deposition on tungsten between molecular dynamics and dynamic Monte Carlo simulation, Surf. Coat. Tech. 202 (2008) 5374–5378.
[26] A. Lasa, C. Björkas, K. Vörtler, K. Nordlund, MD simulations of low energy deuterium irradiation on W, WC and W2C surfaces, J. Nucl. Mater. 429 (2012) 284–292.
[27] K. Ohya, Y. Kikuhara, K. Inai, A. Kirschner, D. Borodin, A. Ito, H. Nakamura, T. Tanabe, Simulation of hydrocarbon reflection from carbon and tungsten surfaces and its impact on codeposition patterns on plasma facing components, J. Nucl. Mater. 390–391 (2009) 72–75.
[28] S.J. Plimpton, Fast parallel algorithms for short-range molecular dynamics, J. Comp. Phys. 117 (1995) 1. http://lammps.sandia.gov.
[29] N. Juslin, P. Erhart, P. Träskelin, J. Nord, K.O.E. Henriksson, K. Nordlund, E. Salonen, K. Albe, Analytical interatomic potential for modeling nonequilibrium processes in the W-C-H system, J. Appl. Phys. 98 (2005) 123520.
[30] K. Tokunaga, M. Takayama, T. Muroga, N. Yoshida, Depth profile analyses of implanted deuterium in tungsten by secondary ion mass spectrometry, J. Nucl. Mater. 220–222 (1995) 800–804.

[31] D. Hildebrandt, P. Wienhold, W. Schneider, Mixed-material coating formation on tungsten surfaces during plasma exposure in TEXTOR-94, J. Nucl. Mater. 290–293 (2001) 89–93.
[32] K. Krieger, J. Roth, Synergistic effects by simultaneous bombardment of tungsten with hydrogen and carbon, J. Nucl. Mater. 290–293 (2001) 107–111.
[33] H. Kimura, Y. Nishikawa, T. Nakahata, M. Oyaidzu, Y. Oya, K. Okuno, Chemical behavior of energetic deuterium implanted into tungsten carbide, Fusion Eng. Des. 81 (2006) 295–299.
[34] H.T. Lee, K. Krieger, Simultaneous irradiation of tungsten with deuterium and carbon at elevated temperatures, J. Nucl. Mater. 390–391 (2009) 971–974.
[35] H.T. Lee, K. Krieger, Modeling tungsten and carbon sputtering by carbon at elevated temperatures, Phys. Scripta T138 (2009) 014045.
[36] T. Sizyuk, A. Hassanein, Dynamic analysis and evolution of mixed materials bombarded with multiple ions beams, J. Nucl. Mater. 404 (2010) 60–67.
[37] J.B. Condon, T. Schober, Hydrogen bubbles in metals, J. Nucl. Mater. 207 (1993) 1–24.
[38] V. Alimov, Kh, et al. "Surface morphology and deuterium retention in tungsten exposed to low-energy, high flux pure and helium-seeded deuterium plasmas", Phys. Scr. T138 (2009) (2009) 014048.
[39] W.M. Shu, A. Kawasuso, T. Yamanishi, Recent findings on blistering and deuterium retention in tungsten exposed to high-fluence deuterium plasma, J. Nucl. Mater. 386 (2009) 356–359.
[40] Martin. Balden, Et al. "D2 gas-filled blisters on deuterium-bombarded tungsten", J. Nucl. Mater. 414 (1) (2011) 69–72.
[41] Naruaki. Enomoto, Et al. "Grazing-incidence electron microscopy of surface blisters in single-and polycrystalline tungsten formed by H+, D+ and He+ irradiation", J. Nucl. Mater. 385 (3) (2009) 606–614.
[42] K. Schmid, J. Roth, Erosion of high- Z metals with typical impurity ions, J. Nucl. Mater. 313 (2003) 302–310.